JOURNAL OF MATERIALS SCIENCE 29 (1994) 5302–5308

Generalized Maxwell–Wagner response in dispersive silver borophosphate glasses

N. U. HAQUE, R. A. HASHMI, M. K. ANIS, N. BANO
Department of Physics, University of Karachi, University Road, Karachi 75270, Pakistan
R. M. HILL*
**Department of Physics, King's College London, The Strand, London WC2R 2LS, UK*

The dielectric response of a glass-forming system ($Ag_2O : B_2O_3 : P_2O_5$) has been measured in the frequency range from 10^{-3}–10^5 Hz and over temperatures in the range 150–400 K for three different compositions. The dynamic behaviour of the conductance and capacitance in these glasses has been observed to follow fractional power-law dependencies on frequency which obey the generalized Maxwell–Wagner relationships. The power-law dispersions for the bulk and the surface layer of the non-ideal solid electrolyte $0.6Ag_2O$: xB_2O_3: $(0.4 - x)$ P_2O_5 have been modelled mathematically using frequency-dependent resistive and capacitive elements in a conventional equivalent network. It is shown that controlled substitution of B_2O_3 in the glassy network influences the response and introduces an imperfect charge transport, the quasi-d.c. process of limited charge transport in place of bulk conduction, at higher frequencies, and affects the diffusion barrier at the electrodes to make them, weakly, more conductive at the lowest frequencies. The magnitudes of the activation energies of conduction indicate thermally activated localized hopping of silver ions between neighbouring sites in a structure that is modified by the addition of boron oxide.

1. Introduction

Ion-conducting glasses have been extensively studied owing to their potential applications as solid electrolytes for solid-state batteries [1–10]. The electrical properties of these glasses have been, in the main, characterized in terms of a d.c. conductivity and the relaxation of that conductivity [1–12]. In practice, the measurement of the conductivity and its relaxation requires the measurement of the complex capacitance, or permittivity, over a wide range of frequencies. The complex capacitance, $C(\omega)$, permittivity, $\varepsilon(\omega)$, susceptibility, $\chi(\omega)$, and conductivity, $\sigma(\omega)$, are related by

$$C(\omega) = C'(\omega) - iC''(\omega) \quad (1a)$$

$$= \frac{A\varepsilon_0}{d}[\varepsilon'(\omega) - i\varepsilon''(\omega)] \quad (1b)$$

$$= \frac{A\varepsilon_0}{d}[\chi'(\omega) + \varepsilon(\infty) - i\chi''(\omega)] \quad (1c)$$

and

$$\sigma(\omega) = \omega\varepsilon_0[\varepsilon''(\omega) + i\varepsilon'(\omega)] \quad (1d)$$

where ε_0 is the absolute permittivity of vacuum, 8.854×10^{-12} F m^{-1}; $\varepsilon(\infty)$ is the infinite frequency permittivity, A is the area of each electrode in a plane parallel electrode geometry, d the equivalent electrode spacing, $i = (-1)^{1/2}$ and the capacitance, permittivity, susceptibility and conductivity are all complex and, in general, dependent on the radian frequency, ω. A number of simple theoretical relationships has been proposed to deal with the conduction processes taking place in glasses [1–12]. These analytical expressions are based on non-dispersive conduction models, with the charge transport independent of frequency. In the simplest of these models, the conductivity process is visualized as a series of consecutive and independent hops of ions over potential barriers along the direction of the electric field [13] and a charge-blocking barrier at each electrode. The capacitance and conductance in this model are independent of frequency so that the sample response can be modelled by a parallel combination of a resistance, R_b and a capacitance, C_b, in series with the capacitance of the barrier regions, C_p. The total impedance of this circuit is given by the sum of the impedances of the barrier and the bulk. Using the impedance to capacitance transformation

$$C(\omega) = [i\omega Z(\omega)]^{-1} \quad (2a)$$

the complex capacitance can be determined as

$$C(\omega) = \frac{C_p(1 + i\omega C_b R_b)}{[1 + i\omega R_b(C_p + C_b)]} \quad (2b)$$

In the particular case when the impedance of the bulk is totally real, R_b, and that of the barrier is purely imaginary, $(i\omega C_p)^{-1}$, Equation 2b reduces to

$$C(\omega) = C_p\frac{1 - i\omega\tau}{1 + \omega^2\tau^2} \quad (3)$$

*Author to whom all correspondence should be addressed.

0022–2461

with $\tau = R_b C_p$. Equation 3 is the Maxwell–Wagner [14, 15] response and is of the Debye relaxation [16] form. We note that the Debye form in capacitance results from a series connection of resistive and capacitive elements and that the equivalent Debye form in terms of dielectric modulus indicates a parallel connection of the same elements. Recently, it has been shown [17, 18] that the dielectric response of solids and liquids departs significantly from the ideal Debye behaviour of Equation 3. Similarly, the perfect Maxwell–Wagner behaviour is seldom observed experimentally in solids, although it might be expected for liquids which contain ionic charge carriers and exhibit perfect charge blocking at the electrodes.

On consideration of experimental results for a wide range of materials [17, 18], Hill and Pickup have suggested [19] that it is possible to construct equivalent networks which represent a range of materials by using frequency-dispersive circuit elements. In this way one can develop analytical expressions for the dielectric response which qualitatively, and quantitatively, fit the experimentally observed behaviour. In the earlier studies [18–20] the dielectric response of materials in terms of bulk and surface layers has been considered by using a dispersive capacitance, C_n, in series with an ideal non-dispersive bulk resistance, R_o. The dispersive nature of the experimental results reported here indicate the necessity for a dispersive resistance, as well as a dispersive capacitance in the equivalent Maxwell–Wagner circuit, a model characterized by Hill and Pickup [19].

The purpose of this work was to explore the validity of the expressions for the complex capacitance of a dispersive system. The system chosen for the present investigation was that of the silver borophosphate glasses the electrolytic and electrochromic properties of which have been, and are, of interest [10]. A brief description of the effects of dispersive capacitive and resistive components will be given, followed by an outline of the theoretical background of a number of dielectric response models. Finally, an analysis of our measurements on a set of three glasses measured over a range of temperatures is presented.

2. Dispersive processes

2.1. Quasi-direct current conduction, the Q-d.c. process

In order to deal with the experimentally observed low-frequency dispersive phenomena, a theory of quasi-direct current conduction (Q-d.c.) has been developed by Dissado and Hill [20] on the basis of many body interactions [21] of mobile charges in the bulk of materials. The model considers an incomplete transport of charge through limited paths between the electrodes. As the charges are limited from moving freely they cause an anomalously large frequency-dependent polarization, and hence capacitance, which is the essential feature of the Q-d.c. process. Experimentally, it has been observed that log/log plots of capacitance against frequency exhibit parallel traces for the real and imaginary components which are spaced apart in the constant ratio $\tan(p\pi/2)$ where p is less than, but close to unity [18]. This results from a fractional power-law response in the susceptibility of the form

$$\begin{aligned}\chi(\omega) &= \chi'(\omega) - i\chi''(\omega) \\ &= \chi(0)\,(i\omega)^{-p} \\ &= \chi(0)\,(\omega)^{-p}[\cos(p\pi/2) - i\sin(p\pi/2)] \end{aligned} \quad (4)$$

from which

$$C''(\omega)/C''(\omega) = \tan(p\pi/2). \quad (5)$$

When $C(\omega) \gg C(\infty)$, as occurs at low frequencies, Equations 4 and 5 apply directly and the Kramers–Kronig relationships are satisfied. The form of Equation 5 is in contrast to the Debye response for which the comparable relationship to that in Equation 5 is (cf. Equation 3)

$$C''(\omega)\,/C'(\omega) = \omega\tau/(1 + \omega^2\tau^2) \quad (6)$$

which tends to $\omega\tau$ as $\omega \to 0$.

2.2. Imperfect resistance

The simplest extension to the Maxwell–Wagner response outlined in Section 1 is to consider that the capacitance of the barrier layer, C_p, is frequency dispersive with the form contained in Equations 4, i.e. $C_p = C_0(i\omega)^{-p}$. Such a model has been reported elsewhere [18]. The broader generalization which is likely to be suitable for materials in which the bulk charge transport of impedance R_b, can be shown to be dispersive [20], is to consider that *both* C_p and R_b are dispersive, i.e. $C_p = C_0(i\omega)^{-p}$ and $R_b = R_b(i\omega)^{-s}$ with s and p both positive and less than unity.

2.3. Diffusion-barrier layer

A capacitive layer arising in the region of the electrode due to the accumulation of charges is termed an interfacial barrier and will have a greater impedance than the bulk of the sample. These charged barrier layers arise from electrochemical processes which are characterized by the dissociation of ionic species. Transport through the layers is by diffusion of the ionic species back into the bulk of the electrolyte [18]. Such diffusive barriers are a special case of the generalized relationship of Equations 4 and 5 with $p = 0.5$, the Wagner process, which is well known in electrochemistry. From Equation 6 we see that for the particular case of a diffusion-dominated barrier

$$C''(\omega)\,/C'(\omega) = \tan(\pi/4) = 1 \quad (7)$$

so that the log/log traces of the real and imaginary components of the capacitance as a function of frequency, degenerate to a single plot of gradient -0.5.

3. Response models

Here we give illustrative examples of the results of combining frequency-dependent and independent circuit elements in order to show the range of the generalized Maxwell–Wagner response.

3.1. A Q-d.c. element in series with a non-dispersive capacitance

The impedance of a series-connected combination is given by the summation of the individual impedances

$$Z(\omega) = (i\omega C_0)^{-1} + (i\omega C_1)^{n-1} \quad (8a)$$

$$= [C_1(i\omega)^{1-n} + C_0(i\omega)]/[C_0C_1(i\omega)^{2-n}] \quad (8b)$$

From which we have that the admittance is given by

$$Y(\omega) = [C_0C_1(i\omega)^{2-n}]/[i\omega C_0 + C_1(i\omega)^{1-n}] \quad (8c)$$

and hence

$$C(\omega) = C_0/[C_1 + C_0(i\omega)^{1-n}] \quad (8d)$$

The response contained in Equation 8d is of the Davidson–Cole type [22] and is shown in Fig. 1a.

3.2. The generalized Maxwell–Wagner model with dispersive elements

For convenience, we use two unit magnitude dispersion functions, $C_s = (i\omega)^{-s}$ and $C_p = (i\omega)^{-p}$, so that the transition occurs at the frequency $\omega = 1$. The equivalent circuit and a typical calculated response are shown in Fig. 1b. With the addition of a constant high-frequency capacitance, C_∞, the algebraic solutions for the real and imaginary components of the capacitance are

$$C'(\omega) = \frac{\omega^p\cos(1/2p\pi) + \omega^s\cos(1/2s\pi)}{\omega^{2p} + \omega^{2s} + 2\omega^{s+p}\cos[1/2(p-s)\pi]} + C_\infty \quad (9a)$$

$$C''(\omega) = \frac{\omega^p\sin(1/2p\pi) + \omega^s\sin(1/2s\pi)}{\omega^{2p} + \omega^{2s} + \omega^{p+s}\cos[1/2(p-s)\pi]} \quad (9b)$$

This dielectric response function has been found to be identical to that which we have observed in our experimental investigation, as we shall show in Section 6. The relationships contained in Equations 9 give the correct limiting behaviour as ω approaches zero or infinity, but the region of principal interest is just above $\omega = 1$ and can best be explored by means of computation.

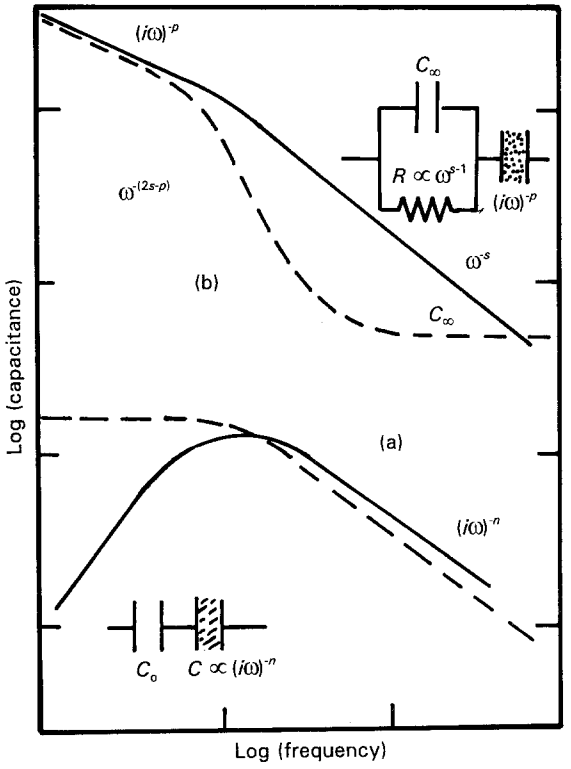

Figure 1 Schematic representation of the generalized Maxwell–Wagner responses. (a) A fractional power-law dispersive element in series with a non-dispersive capacitance. At high frequencies the parallel behaviour of the Q-d.c. element dominates but is truncated by the constant capacitance at low frequencies. The response is of the form of a Cole–Davidson plot. (b) Generalized Maxwell–Wagner plot. The blocking capacitance in (a) is now dispersive with exponent $-p$ and as $s \to 1$ the imaginary component of the high-frequency element acts as a conductance, whilst the real component assumes an exponent of magnitude $2s - p$. Note that this exponent reverts to a value of 2, the classic Maxwell–Wagner value, when s is unity and p is zero.

4. Experimental procedure

Three glasses based on the composition $0.60Ag_2O + xP_2O_5 + (0.40 - x)B_2O_3$ with $x = 0.40$, 0.36 and 0.28, were prepared using a conventional quenching technique. X-ray diffraction analysis confirmed the amorphous nature of these glasses. To make electrical measurements, gold electrodes were evaporated on both sides of the pellets in a vacuum of better than 10^{-5} torr (1 torr = 133.322 Pa). The dielectric measurements were carried out using a Solartron 1255 Frequency Response Analyser (FRA) coupled to a Chelsea Dielectric Interface through an Opus-V PC, a Roland DXY-880 plotter and an Oxford DN 1704 Cryostat with an ITC4 temperature controller. The experimental procedure was the same as that reported earlier by Anis and co-workers [23, 24].

5. Results

All the experimental data are presented in the form of log/log plots of the real, $C'(\omega)$, and imaginary, $C''(\omega)$, components of capacitance as functions of the frequency (Hz) in order to give a clear presentation of the fractional power-law behaviour observed. We use capacitance as the reported property because the presence of barriers in the system does not allow the use of a bulk property such as permittivity. Furthermore, the capacitance has been measured to a higher degree of accuracy than it is possible to determine the ratio A/d for the cast samples. Fitting of the experimental data to simple circuit networks of a frequency-dependent capacitance of fractional power law form, a Q-d.c. process and a dispersive resistance has been carried out making use of a computer program in order to obtain rapid fitting of the observed responses. The exponent values can be determined to better than 3% as indicated in Table I.

The principal feature of our experimental results is the presence of a strong dispersion in the capacitance $C'(\omega)$ which we attribute to a barrier effect in the region of the electrodes and which gives rise to the

TABLE I The values of the transport exponents

Glass composition	Temp., T (°K)	Exponent			Log[$G(\omega)$]
		s	$2s-p$	p	
Glass 1	200	0.93	1.36	0.50	− 9.83
60% Ag	225	0.94	1.38	0.50	− 7.90
and	250	0.95	1.38	0.52	− 7.20
40% P_2O_5	270	0.96	1.37	0.53	− 6.60
	290	0.97	1.40	0.54	− 5.90
	304	0.98	1.42	0.54	− 5.53
	325	0.99	1.45	0.53	− 4.80
	350	0.99	1.46	0.52	− 4.25
	375	0.99	1.49	0.51	− 3.70
	400	1.00	1.50	0.50	
Glass 2	200	0.80	1.10	0.49	− 8.45
60% Ag_2O,	225	0.82	1.15	0.50	− 7.85
36% P_2O_5	250	0.84	1.18	0.50	− 6.95
and	275	0.86	1.23	0.49	− 5.00
4% B_2O_3	304	0.89	1.26	0.52	− 5.25
	320	0.91	1.32	0.50	− 4.85
	340	0.91	1.33	9.49	− 4.35
	360	0.93	1.34	0.52	− 3.95
	380	0.94	1.34	0.54	− 3.55
	400	0.96	1.37	0.56	− 3.45
Glass 3	200	–	–	–	− 8.25
60% Ag_2O	225	0.80	1.14	0.50	− 7.35
28% P_2O_5	250	0.82	1.16	0.50	− 6.98
and	275	0.85	1.20	0.50	− 5.70
12% B_2O_3	304	0.88	1.24	0.53	− 4.85
	320	0.91	1.30	0.53	− 4.55
	340	0.93	1.34	0.52	− 4.20
	360	0.94	1.38	0.50	− 3.95
	380	0.96	1.42	0.52	− 3.70
	400	0.97	1.40	0.54	− 3.45

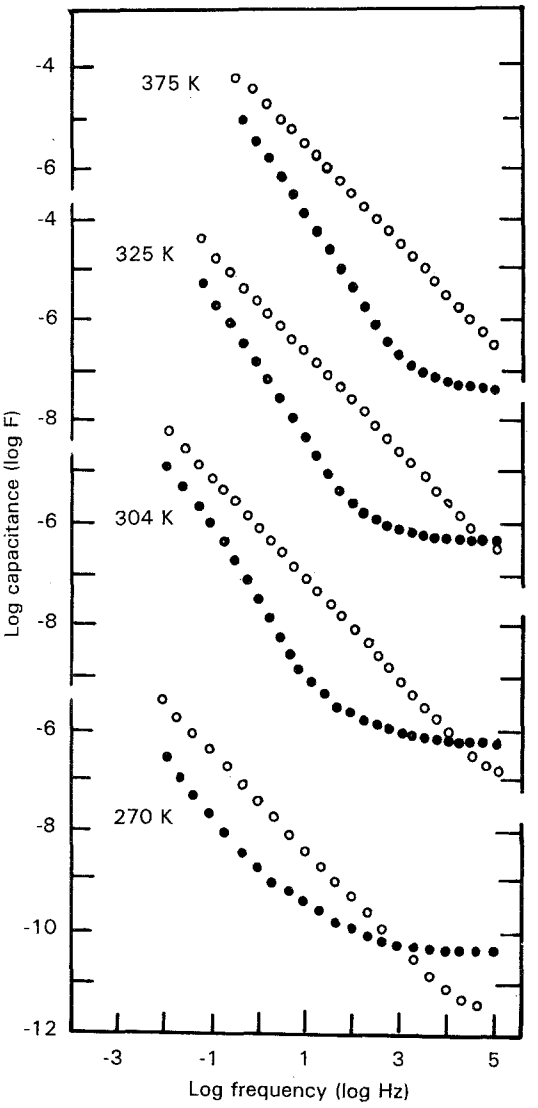

Figure 2 Selected spectral data for Glass 1, zero B_2O_3 content. The temperatures of measurement (K), are indicated and each data set has been displaced in magnitude for clarity. Here, and in Figs 4 and 6, $C(\omega) = C'(\omega) - iC''(\omega)$ with (○) $C'(\omega)$; (●) $C''(\omega)$.

generalized Maxwell–Wagner response, outlined in Section 3.2. and sketched in Fig. 1b.

As a first example, we present in Fig. 2 the data for the glass of composition $0.60Ag_2O:0.40P_2O_5$, Glass 1. In this figure, the individual data sets which were obtained in the temperature range 270–375 K are displaced in magnitude by three or four decades, for reasons of clarity. The exponent of $C'(\omega)$ is well defined for each data set and gives values for s, listed in Table I, in the range 0.93–1.0. The exponent $2s - p$, which for $C'(\omega)$ in the transition region dominates the frequency region below 100 Hz, is more variable with temperature. Taking the lowest frequency asymptotic gradient gives values in the range 1.3–1.5. These data are shown in Fig. 3 together with the low-frequency barrier exponent, p, which has been determined to be essentially constant at 0.5.

The novel feature of these data is the continuous temperature dependence of s over the range up to 330 K. Above about 380 K, s reaches its maximum value of unity and we observe a non-dispersive conductance in the sample. In the region where s is less than, but close to, unity, charge movement in the glass is of the Q-d.c. type. We note that because of the temperature dependence of s, these data cannot be temperature normalized, as is commonly done with dielectric data [17], because the spectral form of the response is not independent of temperature. As the frequency exponents are related to the degree of order in the structure [20, 21] their temperature dependence is characteristic of a metastable structure in this temperature range.

Equivalent spectral plots for Glass 2 are given in Fig. 4 and the analysis of the exponents in Fig. 5. The small boron oxide component appears to give a more glassy structure in that the exponents have not reached their equilibrium values by 400 K. In contradistinction, however, the low-frequency exponent, p, is reasonably constant at 0.5 at the *lower* temperatures and now increases towards 0.6 for temperatures in excess of 350 K. The rate of change of the transport exponent, s, is surprisingly constant throughout the temperature range investigated, with no apparent saturation as its maximum value of unity is approached. The values of the exponents are listed in Table I.

Figs 6 and 7 present the equivalent information for Glass 3 which shows a reasonably constant value for the barrier exponent at 0.5 throughout the temperature range, but with an indication that it is increasing at the highest temperatures investigated. The exponent s is little changed from that observed in Glass 2,

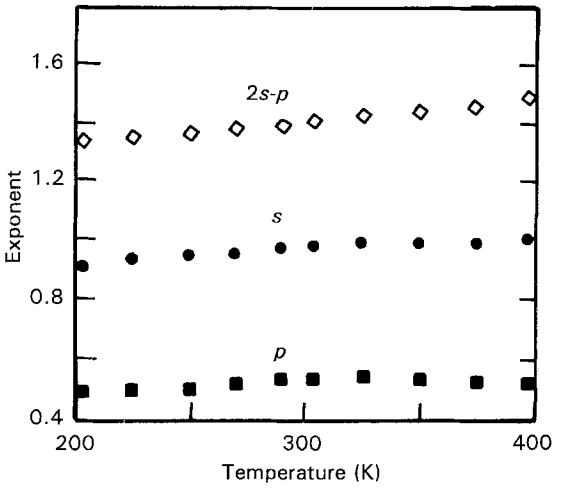

Figure 3 Plots of the measured frequency exponents $2s - p$ and s together with the deduced values of p as functions of temperature for Glass 1. Note that p is essentially constant at 0.5 throughout the temperature range, indicative of the presence of a diffusive barrier at the electrodes.

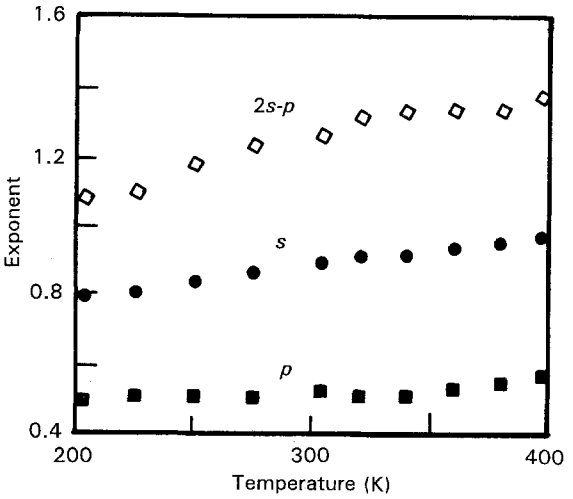

Figure 5 Plots of the measured and derived exponents for Glass 2. In this material p is only constant at the value of 0.5 for temperatures less than 300 K, and the temperature dependence of the exponent, s, is large and constant in the range investigated.

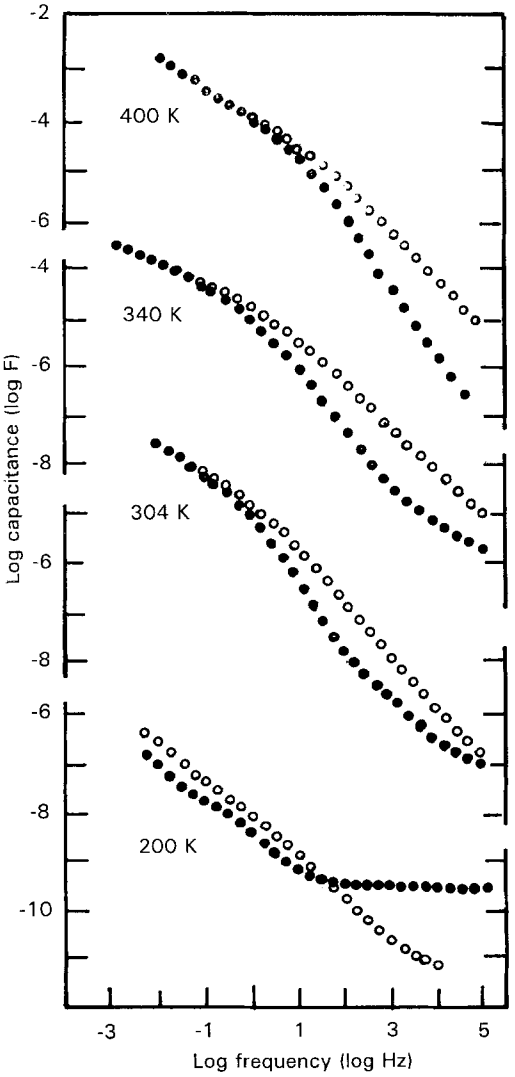

Figure 4 Selected data sets for Glass 2, which contains 4% B_2O_3.

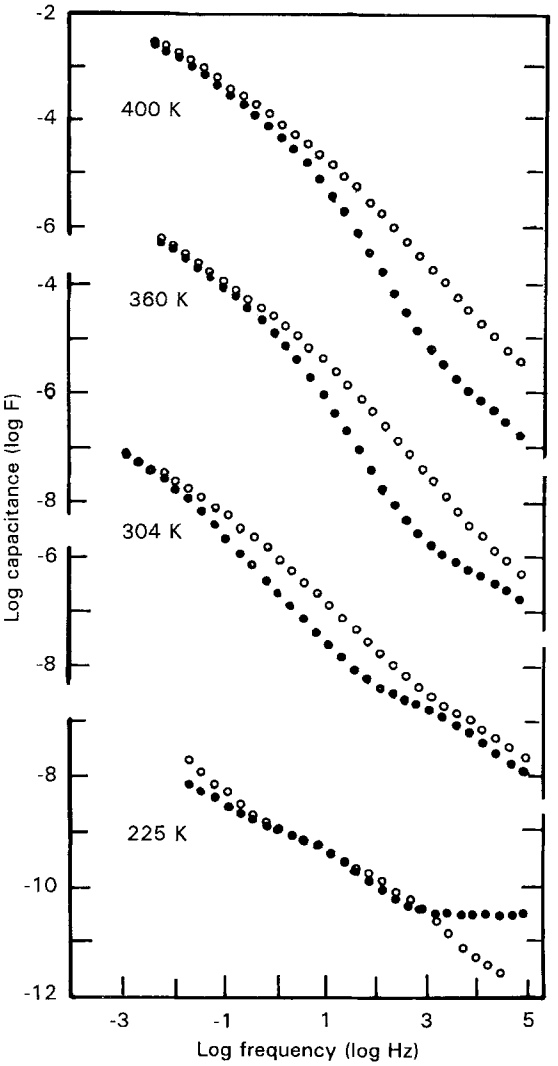

Figure 6 Selected data sets for Glass 3, 12% B_2O_3. The data in the temperature range above 300 K are similar to those obtained for Glass 2 with diffusive behaviour dominating at low frequencies. At the lowest frequency measured, there is some indication of a barrier conductance developing.

in particular, the rate of change of s with temperature has not changed significantly.

Figs 2, 4 and 6 show the detail of the spectral responses. Glasses 2 and 3, particularly at high temperatures and low frequencies, give clear evidence for dispersive barriers which have been deduced from the magnitudes of the higher frequency exponents of C' and C''. In both cases, for measurement temperatures

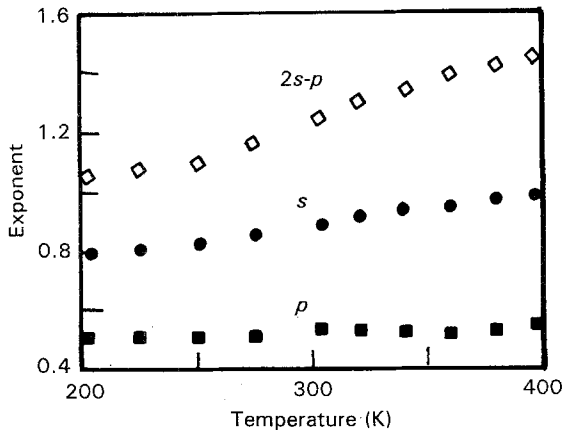

Figure 7 Plots of the measured and derived exponents for Glass 2. The forms of the exponents are almost identical to those determined for Glass 1.

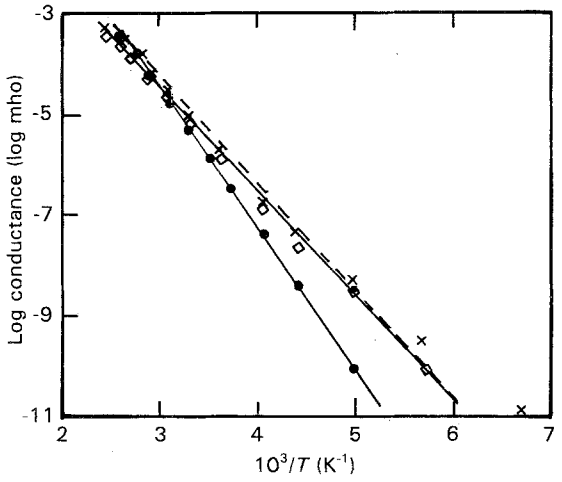

Figure 8 Arrhenius plots of the a.c. conductances of the three glasses at 1 Hz. Note the cross-over in the region of $T^{-1} = 3$. (●) Glass 1, (◇) Glass 2, (×) Glass 3.

TABLE II The acitivation energies indicated by the linear regions of the plots

Glass	Activation energy (eV)
1	0.58
2	0.35
3	0.44

greater than about 300 K, the real and imaginary components of the complex capacitance are of almost equal magnitude, the dispersion characteristic of a perfectly diffusive barrier.

Arrhenius plots of the a.c. conductance at 1 Hz, the lowest limit of the bulk conductance, are given in Fig. 8 and the activation energies indicated by the linear regions of the plots are listed in Table II. The zero boron content glass has the highest activation energy of 0.58 eV, whereas the lowest boron concentration glass has the lowest activation energy and a higher conductance. It can be seen that both the boron glasses have similar conductance values and hence we could deduce that the addition of boron induces easier transport in the glassy structure but does not add significantly to the density of the carriers. Indeed, we note that the infinite temperature conductance of the non-boron containing glass would be significantly higher than that for those containing boron, and hence we can deduce that the density of carriers has to be less than in Glass 1, but that the mobilities are greater.

6. Conclusion

Three low-conductivity glasses based on a silver oxide–phosphorous oxide system to which boron oxide has been added have been examined dielectrically in the frequency range 10^5–10^{-3} Hz as functions of temperature. It has been observed that *all* the glasses form a charge diffusive layer at the electrodes and comparison of the relative magnitudes of the barrier capacitance with the high-frequency capacitance indicates a thickness for the barrier layers that is of the order of 10^{-5} of the sample thickness, i.e. about 10 nm.

In the bulk of the glass, the undoped material exhibited a well-defined conductance, $s \rightarrow 1.0$, at temperatures in excess of 300 K. In all other cases, the bulk charge transport was of the form of a Q-d.c. process in which a significant fraction of the mobile charge becomes trapped in the structure. It has been shown that the series combination of bulk charge transport and diffusive barriers gives a generalized Maxwell–Wagner response; however, in the case of the samples reported here, the barriers are not perfectly dispersive and the exponent of the bulk transport is, in general, temperature dependent. Hence not only do we deduce that the glassy structures are metastable, but they develop towards the more ordered form at higher temperatures.

Consideration of the temperature dependencies of the a.c. conductance as a function of temperature indicates that the density of charge carriers is largest for the boron-free glass, but that the mobility of these carriers is low due to charge trapping and exhibits a relatively high activation energy. Conversely, the doped material has lower activation energy for transport but fewer charge carriers. The formation of the diffusive charge barriers would suggest that the carriers are ionic in nature with a low efficiency for charge exchange at the electrodes.

In conclusion, we deduce that the effect of adding significant concentrations of B_2O_3 to the silver phosphate glass has not changed the basic dielectric response of a bulk conduction process in parallel with a constant, bulk, capacitance, the two being in series with electrode barrier layers. It has, however, strengthened the diffusive nature of the barrier layers and decreased the efficiency of charge transport in the bulk whilst decreasing its activation energy. From this information we deduce that the boron has contributed carriers to the system and that these carriers are less deeply bound than in the undoped material. We have determined, through the dispersive exponent, s, that the physical structures of the doped materials are

metastable over the temperature range from 200–400 K. As, at the highest temperatures, s is approaching its maximum value of unity, we postulate that the structures will become regular and stable above a temperature of about 425 K. We note that at the lowest temperatures, the glass with the higher doping, Glass 3, exhibits a decreasing activation energy. This can be taken as evidence for impurity conduction becoming dominant at low temperatures.

References

1. C. A. ANGELL, *Solid State Ionics* **9/10** (1983) 3.
2. J. L. SOUQUET, *Ann. Rev. Mater. Sci.* **11** (1981) 211.
3. T. MINAMI, *J. Non-cryst. Solids* **56** (1983) 15.
4. J. P. MALUGANI and G. ROBERT, *Mater. Res. Bull.* **14** (1979) 1075.
5. H. S. MAITI, A. R. KULKARRNI and A. PAUL, *Solid State Ionics* **9/10** (1983) 605.
6. M. RIBES, D. RAVAINE, J. L. SOUQUET and M. MAURIN, *Rev. Chem. Mineral* **16** (1979) 339.
7. M. RIBES, D. RAVAINE and J. L. SOUQUET, *J. Non-Cryst. Solids* **38/39** (1980) 271.
8. S. W. MARTIN and C. A. ANGELL, *J. Am. Ceram. Soc.* **67** (1984) c-148.
9. *Idem, J. Non-Cryst. Solids* **66** (1984) 429.
10. A. MAGISTRIS and G. CHIODELLI, *Solid State Ionics* **9/10** (1983) 611.
11. P. B. MACEDO, C. T. MOYNIHAN and R. BOSE, *Phys. Chem. Glasses* **13** (1972) 171.
12. J. M. STEVELS, *J. Non-Cryst. Solids* **73** (1985) 165.
13. D. P. ALMOND and A. R. WEST, *Solid State Ionics* **11** (1983) 57.
14. J. C. MAXWELL, "Treatise on Electricity and Magnetism", 3rd Edn (Dover Press, New York, 1954).
15. R. J. WAGNER, *Ann. Physik.* **40** (1913) 317.
16. P. DEBYE, "Polar Molecules" (Dover Press, New York, 1945).
17. R. M. HILL, *J. Mater. Sci.* **16** (1981) 118.
18. A. K. JONSCHER, "Dielectric Relaxation in Solids" (Chelsea Dielectrics Press, London, 1983).
19. R. M. HILL and C. PICKUP, *J. Mater. Sci.* **2** (1985) 4431.
20. L. A. DISSADO and R. M. HILL, *J. Chem. Soc. Farad. Trans.* **280** (1984) 291.
21. *Idem, Proc. R. Soc.* **A390** (1983) 131.
22. D. W. DAVIDSON and R. H. COLE, *J. Chem. Phys.* **19** (1951) 1484.
23. M. K. ANIS, R. A. HASHMI, S. N. Y. BUKHARI and S. A. ANSARI, *Jpn J. Appl. Phys.* **31** (1992) 1825.
24. M. K. ANIS, R. A. HASHMI, M. U. SHAHRUKH and M. SAHBA, *Phys. B* **179** (1992) 278.

Received 23 February
and accepted 10 May 1994